I R I D E

Interdisciplinary Research Infrastructure with Dual Electron linacs&lasers

Massimo.Ferrario@lnf.infn.it
on behalf of

D. Alesini[1], M. P. Anania[1], M. Angelone, D. Babusci[1], A. Bacci[3], A. Balerna[1], M. Bellaveglia[1], M. Benfatto[1], R. Boni[1], R. Bonifacio[7], M. Boscolo[1], F. Bossi[1], B. Buonomo[1], M. Castellano[1], L. Catani[4], M. Cestelli-Guidi[1], V. Chiarella[1], A. Clozza[1], A. Cianchi[4], R. Cimino[1], F. Ciocci[14], E. Chiadroni[1], C. Curceanu[1], S. Dabagov[1], G. Dattoli[14], P. De Felice[5], G. Delle Monache[1], D. Di Gioacchino[1], D. Di Giovenale[1], E. Di Palma[14], G. Di Pirro[1], A. Doria[14], U. Dosselli[1], A. Drago[1], A. Esposito[1], R. Faccini[2], M. Ferrario[1], G. P. Gallerano[14], A. Gallo[1], M. Gambaccini[11], C. Gatti[1], G. Gatti[1], A. Ghigo[1], L. Giannessi[14], F. Giorgianni[2], E. Giovenale[14], C. Guaraldo[1], R. Gunnella[8], S. Ivashyn[12], S. Loreti[5], S. Lupi[2], A. Marcelli[1], C. Mariani[16], M. Mattioli[2], G. Mazzitelli[1], P. Michelato[3], M. Migliorati[2], C. Milardi[1], E. Milotti[13], S. Morante[4], D. Moricciani[2], A. Mostacci[2], V. Muccifora[1], P. Musumeci[10], E. Pace[1], C. Pagani[3], V. Palmieri, L. Palumbo[2], M. Pedio, A. Perrone[9], A. Petralia[14], V. Petrillo[3], P. Pierini[3], A. Pietropaolo, M. Pillon, R. Pompili[4], C. Quaresima[15], L. Quintieri[5], J. V. Rau, C. Ronsivalle[14], J. B. Rosenzweig[10], A. A. Rossi, A. R. Rossi[3], E. Sabia[14], L. Serafini[3], D. Sertore[3], O. Shekhovtsova[12], I. Spassovsky[14], T. Spadaro[1], B. Spataro[1], V. Surrenti[14], A. Tenore[1], A. Torre[14], C. Vaccarezza[1], A. Vacchi[13], P. Valente[2], G. Venanzoni[1], S. Vescovi[1], F. Villa[1], N. Zema[15], M. Zobov[1].

I R I D E

Interdisciplinary Research Infrastructure with Dual Electron linac&laser

Massimo.Ferrario@lnf.infn.it

on behalf of

(1) INFN-LNF
(2) INFN and Universita' di Roma"La Sapienza"
(3) INFN and Universita' di Milano
(4) INFN and Universita' di Roma"Tor Vergata"
(5) Istituto Nazionale di Metrologia delle Radiazioni Ionizzanti, ENEA C R Casaccia.
(7) INFN and Universidade Federal da Paraiba, Brazil
(8) Universita' di Camerino
(9) INFN and Universita' del Salento
(10) UCLA, Los Angeles, USA
(11) INFN and Universita' di Ferrara
(12) ITP NSC KIPT, Kharkov, Ukraine
(13) INFN and Universita' di Trieste
(14) ENEA – Frascati
(15) CNR
(16) CNISM and Universita' di Roma"La Sapienza"

- Science with Free Electron Lasers (FEL) from infrared to X-rays,
- Nuclear photonics with Compton back-scattering γ-rays sources,
- Fundamental physics with low energy linear colliders
- Advanced Neutron sources by photo-production,
- Science with THz radiation sources,
- Physics with high power/intensity lasers,

- R&D on advanced accelerator concepts including plasma accelerators and polarized positron sources
- ILC technology implementation
- Detector development for X-ray FEL and Linear Colliders
- R&D in accelerator technology and industrial spin – off

I R I D E is a large infrastructure for fundamental and applied physics research. Conceived as an innovative and evolutionary tool for multi-disciplinary investigations in a wide field of scientific, technological and industrial applications, it will be a high intensity "particle beams factory".

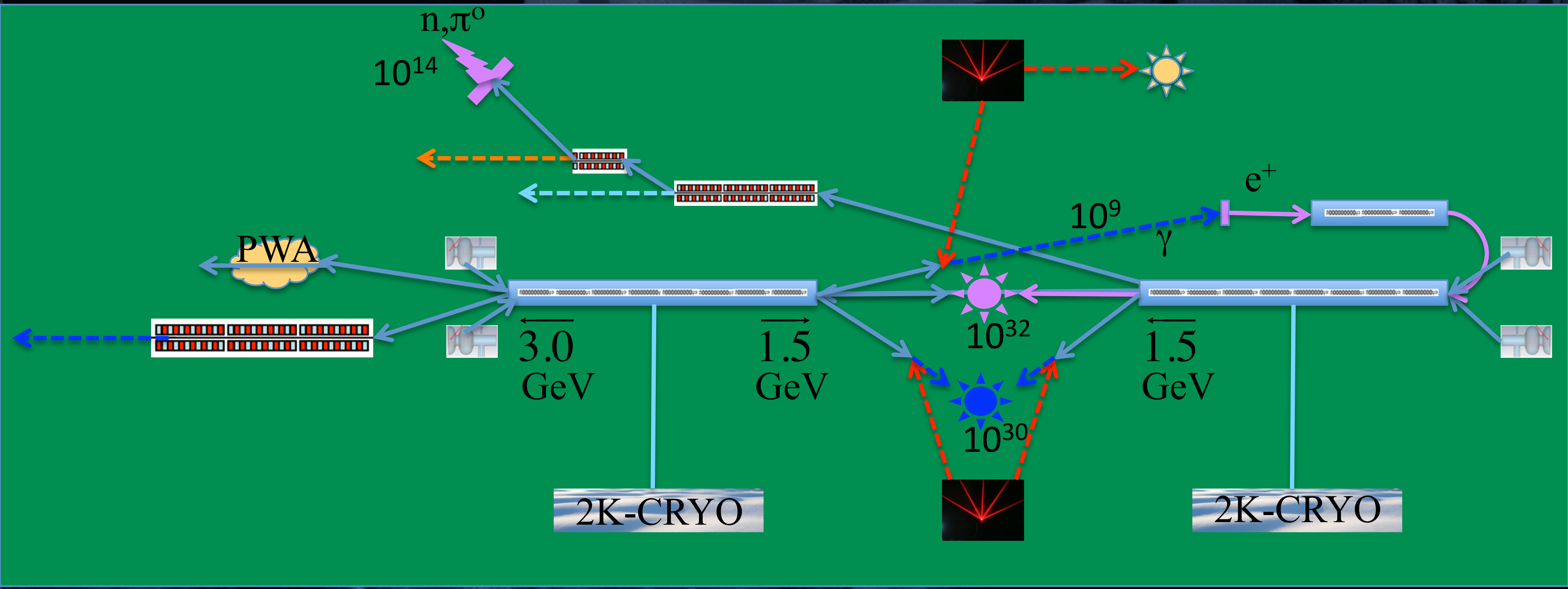

Based on a combination of a high duty cycle radio-frequency superconducting electron linac (SC RF LINAC) and of high energy lasers it will be able to produce a high flux of electrons, photons (from infrared to γ-rays), neutrons, protons and eventually positrons, that will be available for a wide national and international scientific community interested to take profit of the most advanced particle and radiation sources.

The main feature of a SC linac relevant for IRIDE is the possibility to operate the machine in continuous (CW) or quasi-continuous wave (qCW) mode with high average beam power (>1 MW) and high average current (>300 μA).

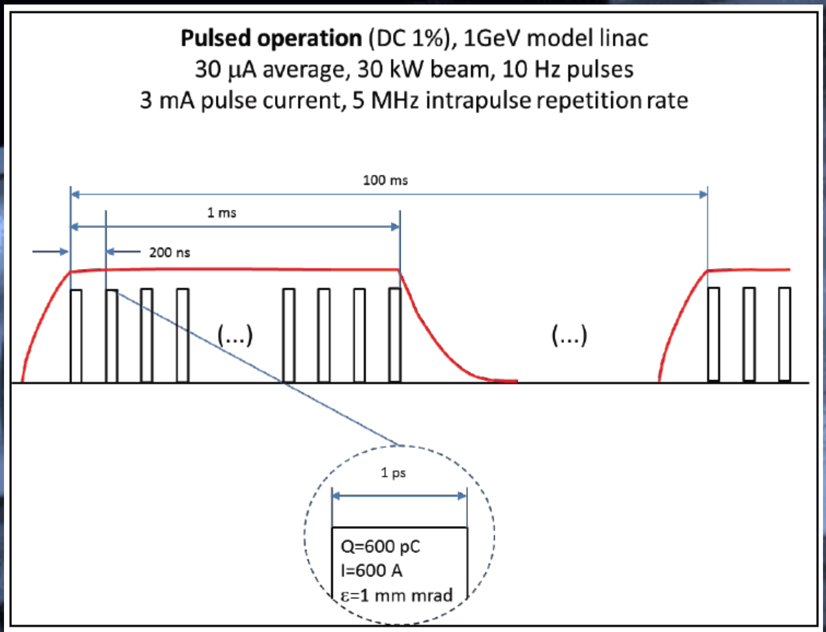

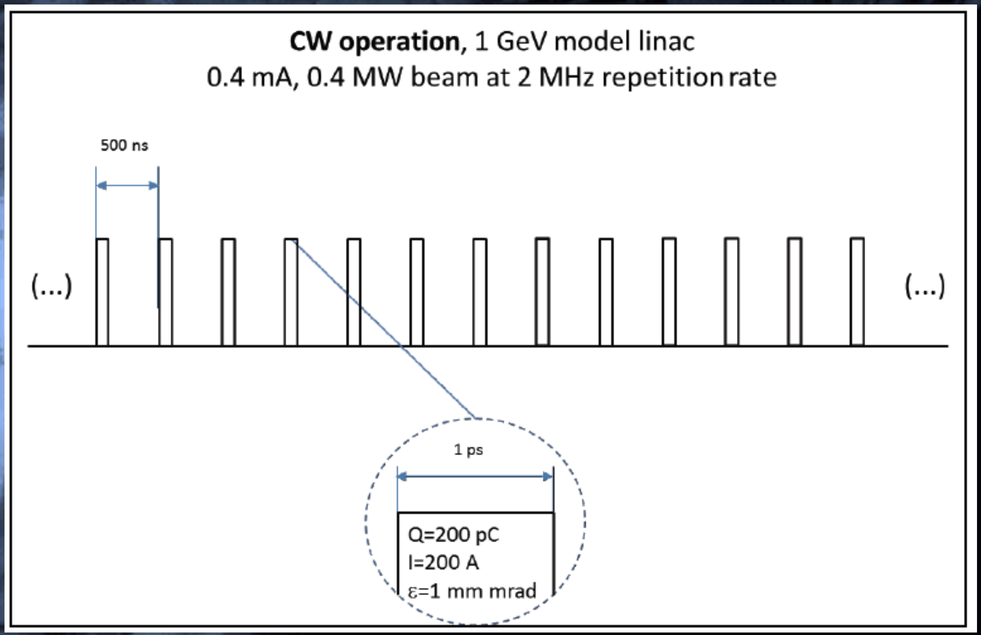

The CW or qCW choice, combined with a proper bunch distribution scheme, offers the most versatile solution to provide bunches to a number of different experiments, as could be envisaged in a multi-purpose facility.

IRIDE LINAC
possible pulsed Configurations (single linac)

$$Q_{ext}^{opt} \approx \frac{V_{acc}}{(R/Q)I_b}$$

$$\frac{P_{ref}}{P_{fwd}} = |\rho|^2 \approx \frac{\left(Q_{ext}^{opt} - Q_{ext}\right)^2}{\left(Q_{ext}^{opt} + Q_{ext}\right)^2}$$

$$V_{asympt} \approx 2\sqrt{(R/Q)Q_{ext}P_{RF}}$$

	Pulse 1	Pulse 2	Pulse 3
E [GeV]	1	1,5	2
I (within pulse) [mA]	4	3	2
I (average) [mA]	0,47	0,28	0,12
Pulse rep. rate [Hz]	100	100	100
RF pulse duration [ms]	1,5	1,5	1,5
RF Duty cycle [%]	15	15	15
Beam pulse duration [ms]	1,16	0,93	0,60
Beam Duty cycle [%]	11,6	9,3	6,0
f_{RF} [MHz]	1300	1300	1300
E_{acc} [MV/m]	7,53	11,29	15,05
Cavity length L [m]	1,038	1,038	1,038
R/Q [Ohm]	1036	1036	1036
Q_0	1,50E+10	1,20E+10	1,00E+10
Q_{ext}_opt	1,89E+06	3,77E+06	7,54E+06
Q_{ext}	3,50E+06	3,50E+06	3,50E+06
Reflected RF power [%]	9,0	0.14	13,5
Cavity BW [Hz]	185,71	185,71	185,71
Cavity rise time [ms]	0,86	0,86	0,86
Rise-time to target V_{acc} [ms]	0,34	0,57	0,90
# of cavies	128	128	128
# of modlules	16	16	16
$P_{beam/}$cavity (pulse) [kW]	31,25	35,16	31,25
P_{beam}/cavity (ave) [kW]	4,69	5,27	4,69
P_{RF}/cavity (pulse) [kW]	34,06	35,20	35,44
P_{RF}/cavity (ave) [kW]	5,11	5,28	5,32
Available P_{RF}/cavity (pulse) [kW]	40,00	40,00	40,00
unloaded asyntotic voltage [MV]	24,09	24,09	24,09
P_{cryo}_RF (@ 2 K) [W]	75,41	212,09	452,46
P_{cryo}_static (@ 2 K) [W]	56,00	56,00	56,00
P_{cryo}_total (@ 2 K) [W]	131,41	268,09	508,46
Total P_{beam} (peak) [kW]	4000	4500	4000
Total P_{beam} (ave) [kW]	465,60	417,95	241,39
Linac length [m]	192	192	192

IRIDE LINAC
possible RF sources

- x 3 pulse duration (from 0.5 to 1.5 ms);
- 1/3 peak power (from 5.1 to 1.7 MW);
- same rep rate (100 Hz) and ave Power (250 kW)

Reasonable but to be verified with manufacturer!

RF performance	TH 2104 C	TH 2104 D	TH 2104 U		
Frequency	1.3	1.3	1.3	GHz	
RF output power					
• peak	5.1	5.1	10.2	MW	
• average	100	250	250	kW	
Peak RF drive power	200	200	320	W	max.
RF pulse duration	2 000	500	250	µs	max.
- 1dB bandwidth	8	8	8	MHz	min.
Saturated gain	47	47	50	dB	typ.
Efficiency	46	45	45	%	typ.

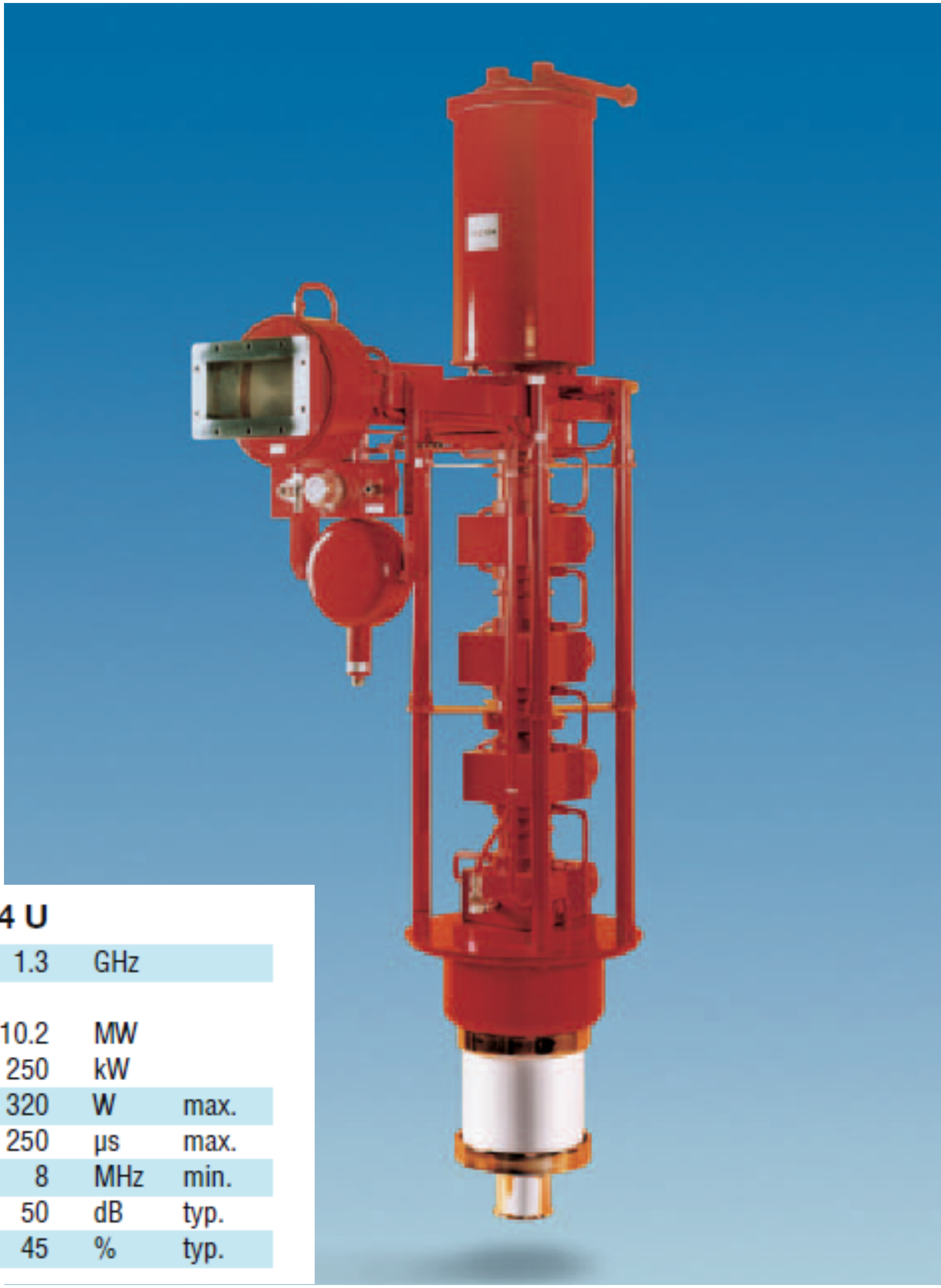

INFN is in a leading position in the SC RF technology, with knowledge and strong capabilities in the design, engineering and industrial realization of all the main component of a superconducting radiofrequency accelerator.

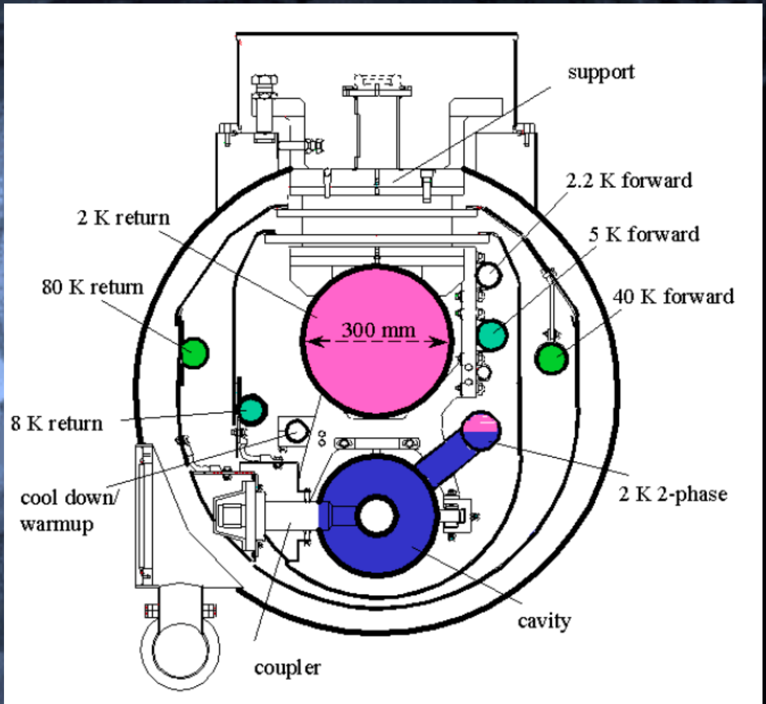

INFN strongly participated to TESLA since the early design stages through the final engineering and shares the know-how and has the recognized intellectual property of several main components one of which is the cryo-module concept and its evolution.

XFEL Italian In-Kind contribution

- **INFN** contributed to linac design
- Italian industry, with INFN supervision provides
  - **400/800** of the 1.3 GHz cavities
    - Fabricated, processed, ready for RF tests
  - **45/100** of the cryomodules
- INFN provides also
  - High QE photocathode preparation/transport system
  - Cavities/Cryomodule for the 3.9 GHz linearizer
- i.e. main components for a **9 GeV SC linac**...

Electron Guns

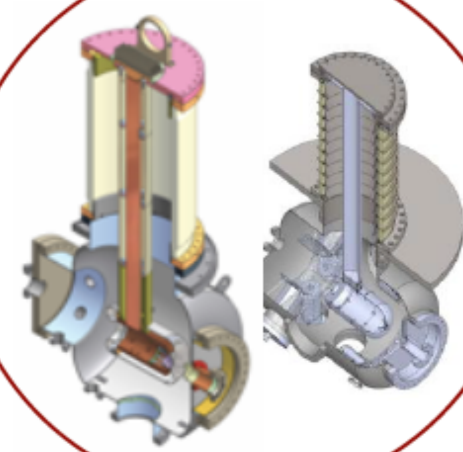

DC guns

+

Hybrid Schemes

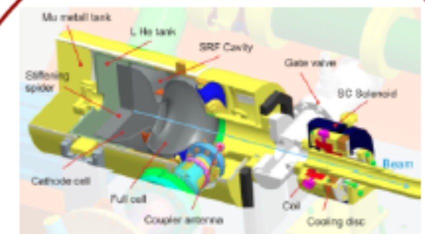

SC RF guns

- CW operation
- High field
- Low pressure
- Low Dark current

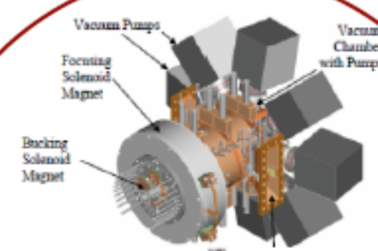

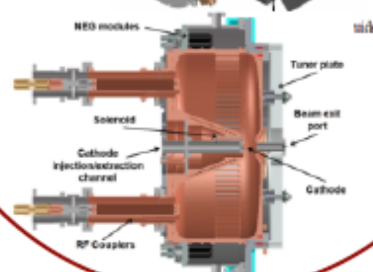

Low freq. (<~ 700 MHz) NC CW RF guns

The LBNL VHF Gun

The Berkeley normal-conducting scheme satisfies all the LBNL FEL requirements simultaneously.

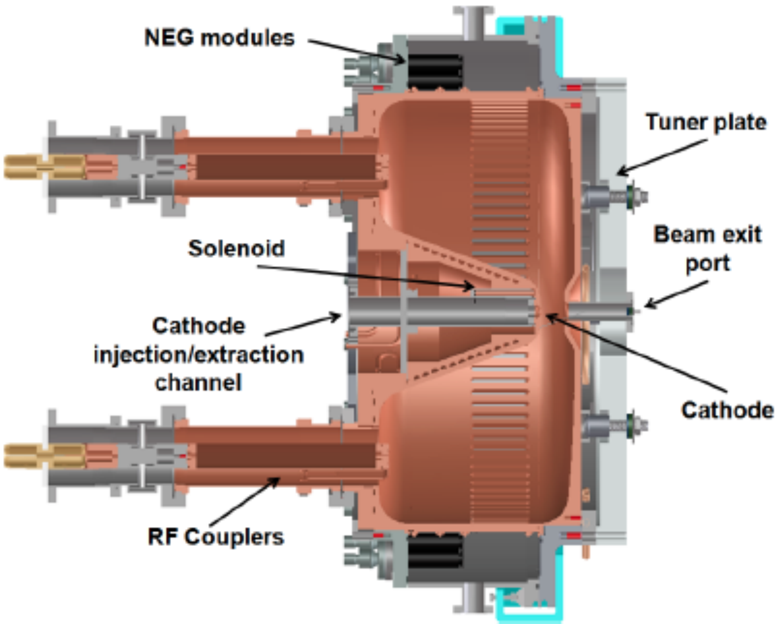

J. Staples, F. Sannibale, S. Virostek, CBP Tech Note 366, Oct. 2006
K. Baptiste, et al, NIM A 599, 9 (2009)

Frequency	186 MHz
Operation mode	CW
Gap voltage	750 kV
Field at the cathode	19.47 MV/m
Q_0 (ideal copper)	30887
Shunt impedance	6.5 MΩ
RF Power	100 kW
Stored energy	2.3 J
Peak surface field	24.1 MV/m
Peak wall power density	25.0 W/cm²
Accelerating gap	4 cm
Diameter/Length	69.4/35.0 cm
Operating pressure	~ 10^{-11} Torr

- At the VHF frequency, the cavity structure is large enough to withstand the heat load and operate in CW mode at the required gradients.
- Also, the long λ_{RF} allows for large apertures and thus for high vacuum conductance
- Based on mature and reliable normal-conducting RF and mechanical technologies.

BERLINpro SCRF

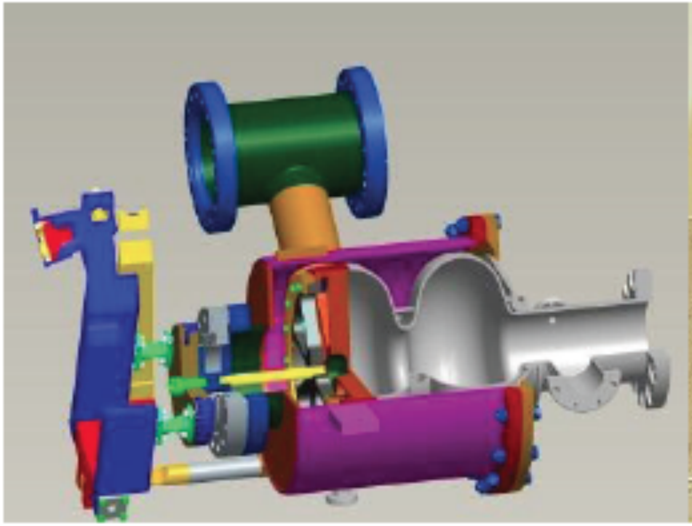

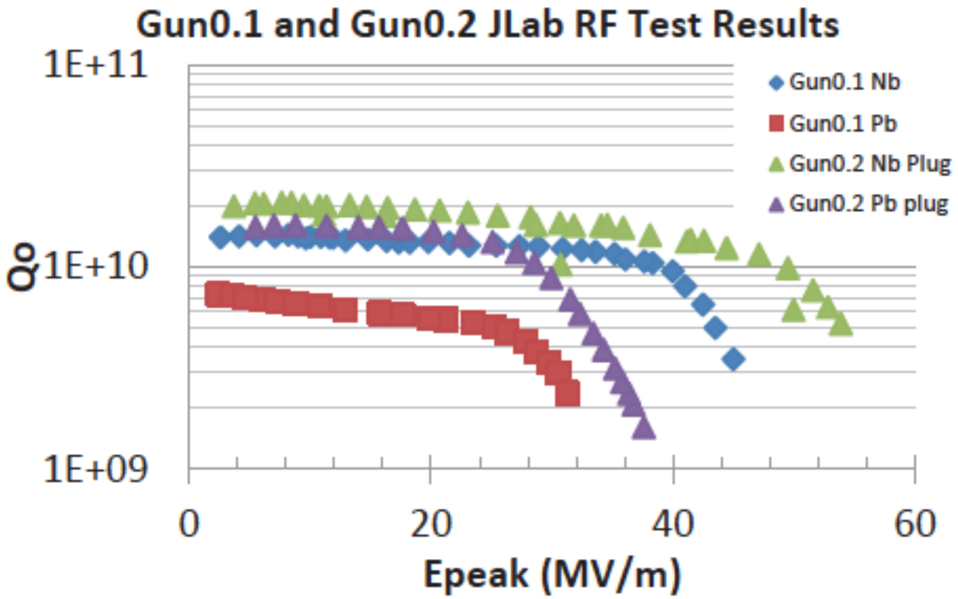

The laser system complex is deputed to deliver optical photon beams able to fulfill the several requirements of the IRIDE facility:

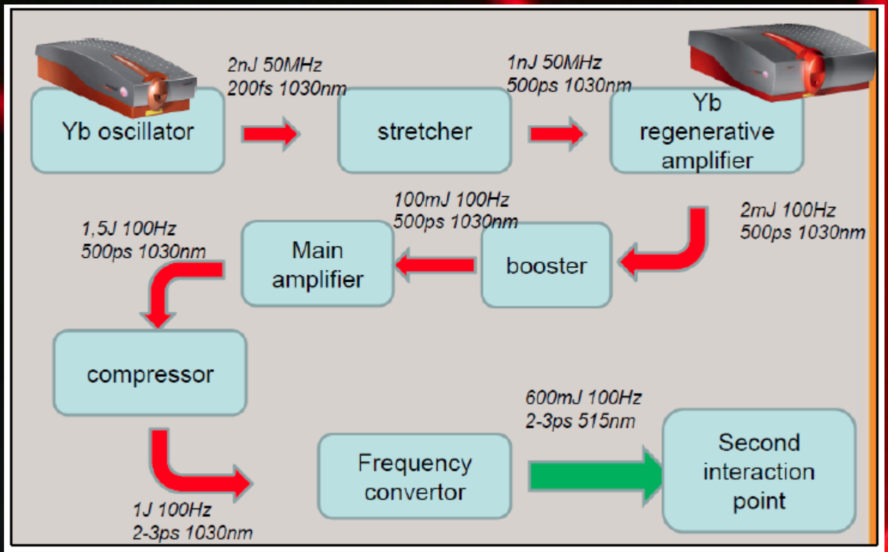

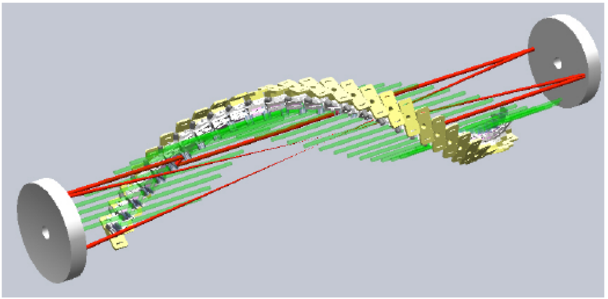
Fig. 133. Schematic view of the re-circulating principle

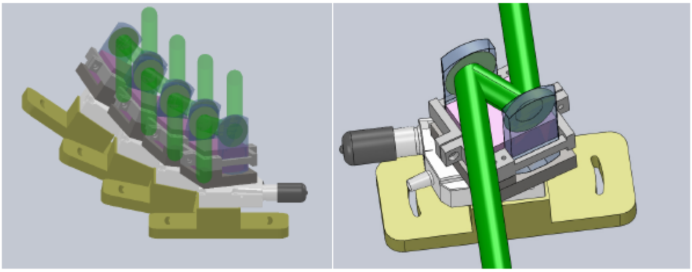
Fig. 134. Schematic view of the motorized mirror pairs used in the re-circulator

- drivers of photo-cathodes for electron beam generation
- colliding laser pulses to drive the back-scattering Compton (Yb:YAG, 100 W, 1 J, 0.1% bw)
- drivers for high advanced acceleration experiments (Ti:Sa, 1 PW, 10^{22} W/cm^2)

Free electron Lasers

The IRIDE project will provide a new concept of FEL facility by merging the two technologies of FEL oscillators and fourth generation radiation sources by developing a facility providing radiation from IR to EUV to the nm region down to Å level using a mechanism of emission already successfully tested at SPARC.

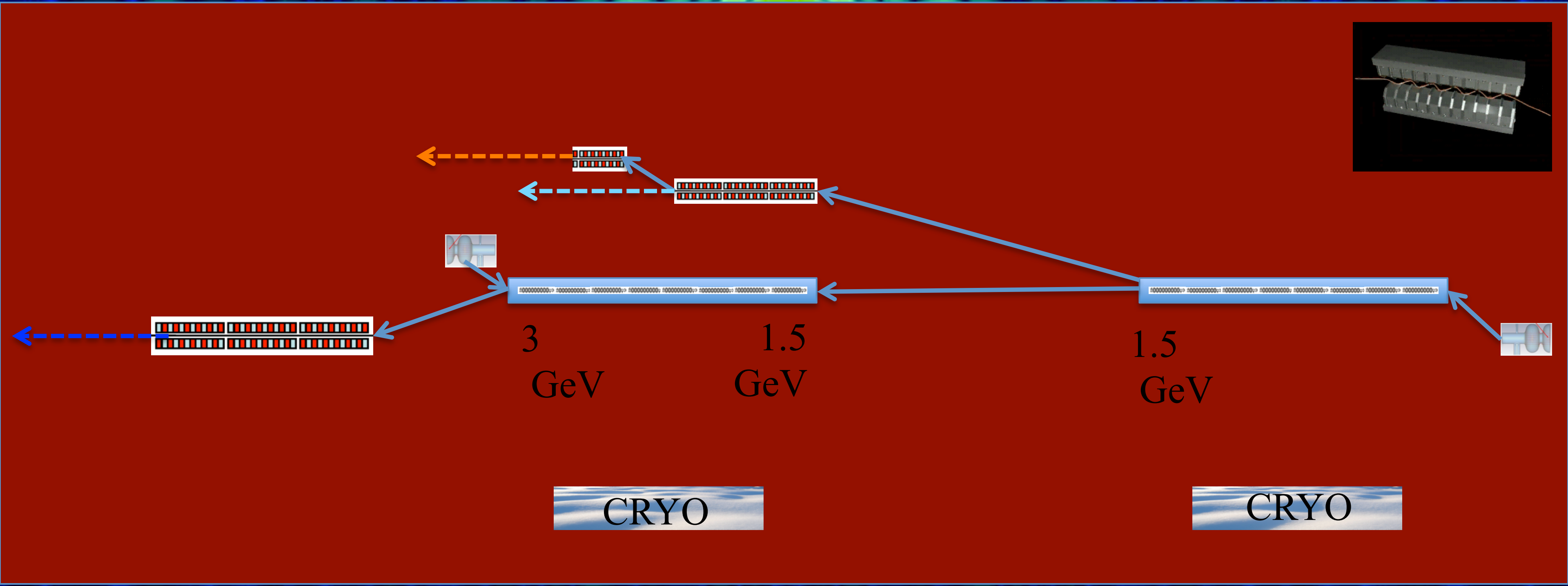

Integrated «architecture»

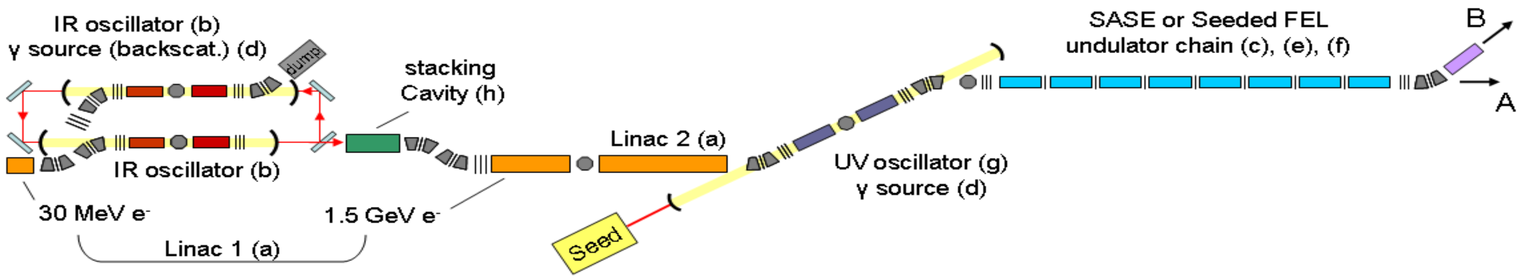

S-C-LINAC structures with 3-4 GeV maximum energy

Between the two Linacs a double FEL oscillator, with a manifold role, is inserted

The undulator chain can be powered by the beam operating at full energy (3-4 GeV) or less

A second FEL oscillator is added for the operation in the UV region and for intra-cavity backscattering for the realization of a gamma source to be exploited for Nuclear Physics studies and the production of polarized electrons

The third FEL section may operate in SASE or SEDEED mode

The seeding will be achieved by exploiting a conventional seeding procedure or by using the self-seeding scheme based on a kind of oscillator-amplifier device, according to the scheme first developed in Barbini et al. "In prospects for 1 Angstrom FEL" Sag Harbor 1990

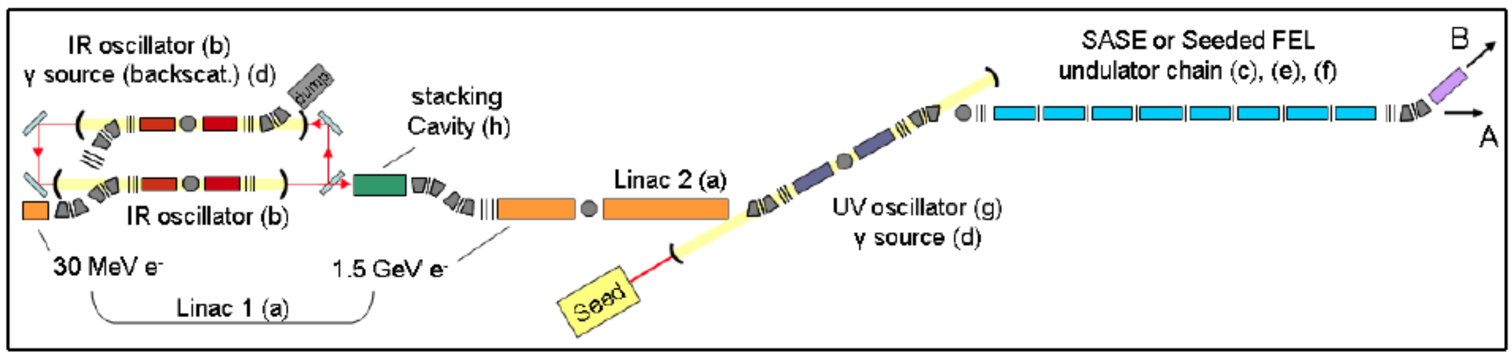

λ(nm/KeV)	1/1.24	0.3/3.72	0.2/6.2
Φ peak (n/s/- 0.1%BW)	$4.6*10^{25}$	$4.1*10^{23}$	$3.4*10^{22}$
B (n/s(mm.mrad)^2 - 0.1%BW)	$6.4*10^{31}$	$5.7*10^{29}$	$4.7*10^{28}$
τ (fs)	220	<200	<180
Φ (n/s) (medio)	$3.95*10^{22}$	$3.51*10^{20}$	$2.89*10^{19}$
photon/bunch	$1.01*10^{13}$	$9.02*10^{10}$	$7.48*10^{9}$

λ(nm/KeV)	4/0.413	1.33/1.23	0.8/2.07
Φ peak (n/s/- 0.1%BW)	$2.7*10^{26}$	$2.5*10^{24}$	$1.9*10^{23}$
B (n/s(mm.mrad)^2 - 0.1%BW)	$1.56*10^{30}$	$1.4*10^{28}$	$1.1*10^{27}$
τ (fs)	95	80	<100
Φ (n/s) (medio)	$1.03*10^{23}$	$9.32*10^{20}$	$7.33*10^{19}$
photon/bunch	$5.94*10^{13}$	$5.5*10^{11}$	$4,18*10^{10}$

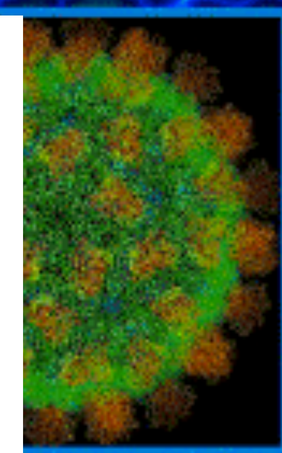

From the SPARX bio-scientific case

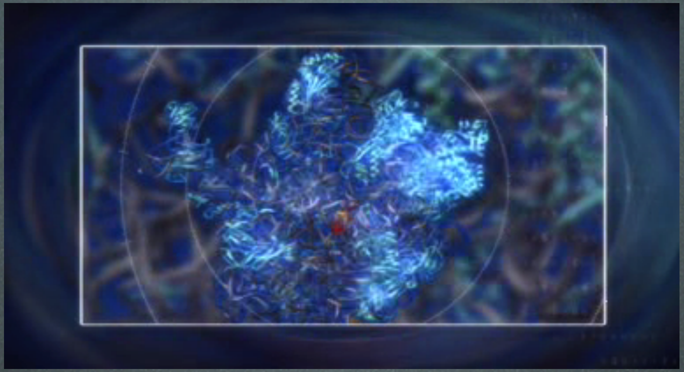

- Time-Resolved diffraction from protein nanochristals with spontaneous radiation: sub-picosecond pumps & probe structural and spectrometric investigations
- Structural characterization of biological systems, muscle contraction
- Small angle X-ray scattering of biological molecules
- Low density Atomic and Molecular processes with two photons spectroscopy
- X-ray microscopy with nanometer resolution
- Femtosecond Raman spectroscopy
- Single molecule imaging with hard X-rays

THz radiation source

The interest for having high-power, sub-ps pulsed radiation covering the spectral range from THz to MIR is rapidly growing, both as it is a powerful tool for investigating the behavior of matter at low energy, and as it allows for a number of possible applications spanning from medical science to security.

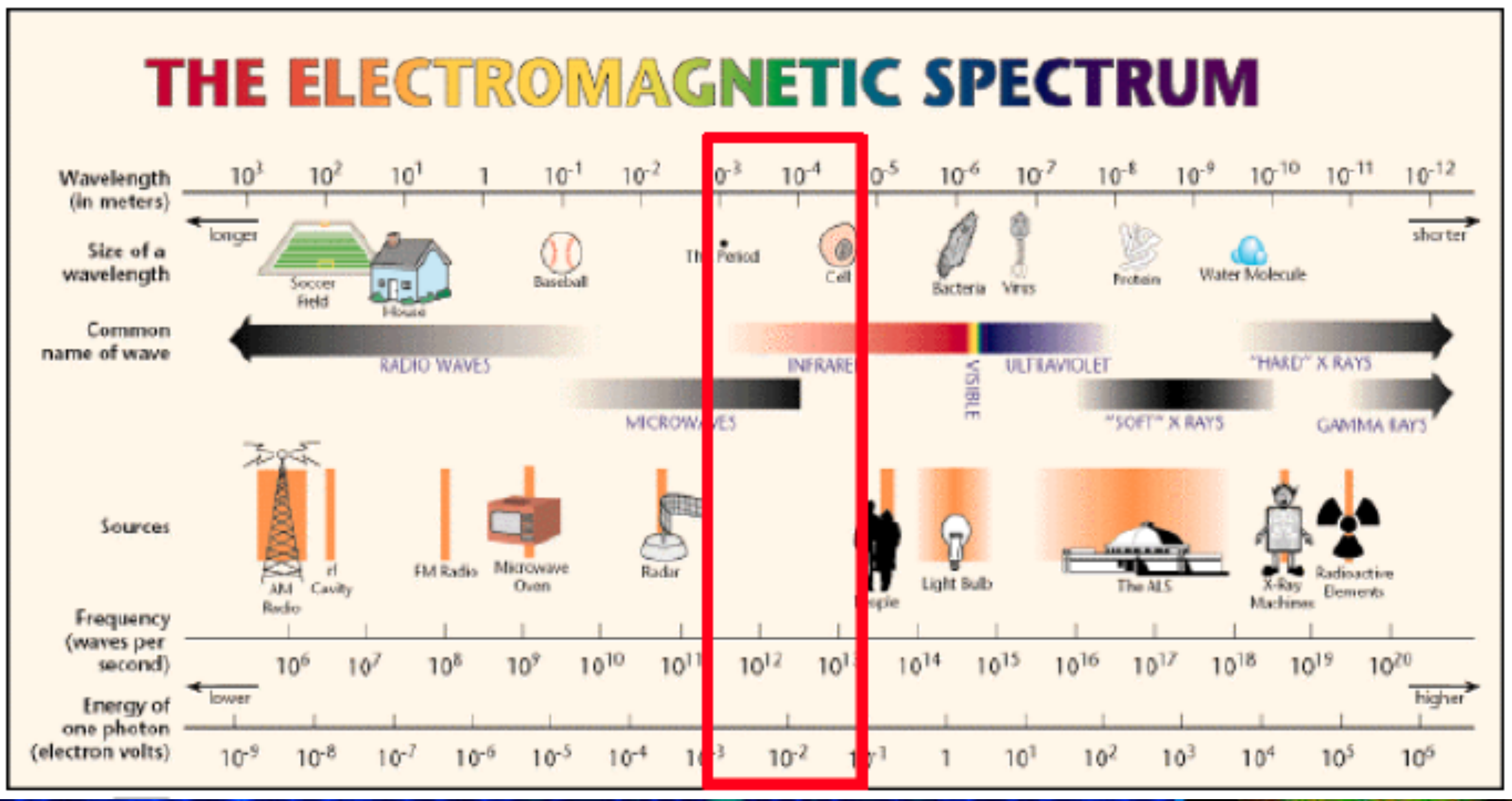

THz radiation source

Condensed Matter Physics

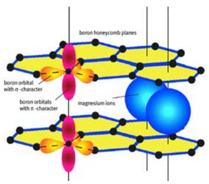

Superconductivity
- Energy gap
- Symmetry of the order parameter
- Direct determination of the superfluid density
- Dynamics of Cooper pairs

Low-dimensional materials
- Dimensionality crossover
- Non-Fermi liquid normal states
- Broken symmetry ground states

Coherent Phase Transitions
- Polarons
- Structural Phase Transitions

Magnetic sub-ps Dynamics

Physical and Analytical Chemistry

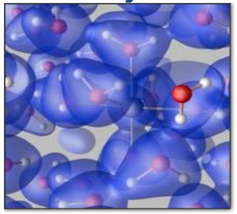

Polar liquids
- Hydrogen bond
- Van der Waals interactions
- Acoustic-Optic phonon mixing in water

Solutions
- Static and dynamic interactions between solvated ions and solvent

Life Sciences

Macromolecules conformation
- Secondary and tertiary structure
- Coherent dynamic development

Imaging
- 3D tomography of dry tissues
- Near-field sub-wavelenght spatial resolution

New Technologies

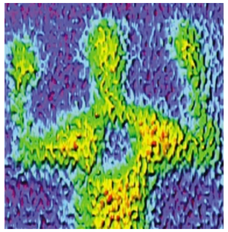

THz technologies
- Array THz detectors
- Metamaterials

Medical diagnostic
- Skin cancer detection

Industrial production
- Material inspection
- Production line monitoring

Defense industry/Homeland security
- Detection of explosives and biohazards

THz radiation source

Electron beam parameters	
Electron energy (GeV)	1.5 – 0.5
Charge/bunch (pC/bunch)	250
RMS bunch length (μm)	60
Normalized emittance (mm mrad)	1
Undulator	
Period (cm)	40
Number of periods	10
Magnetic field (T)	0.1 -1
Coherent Undulator Radiation parameters	
Wavelength (μm)	20 – 200
Peak power (MW)	100
Micropulse energy (mJ)	10
Micropulse duration (fs)	200
Coherent Diffraction Radiation parameters	
Wavelength (μm)	> 60
Peak power (MW)	100
Micropulse energy (μJ)	> 10
Micropulse duration (fs)	200

Neutron Source

A Neutron Source can be realized by photo-production sending high energy electrons on a suitable high Z target. This kind of source allows to obtain neutrons with an energy spectrum that spans over more than 9 decades of energy from few meV up to hundred of MeV, even if most of them have energy around the nuclear equilibrium temperature of the target material (for W, it is around 1 MeV)

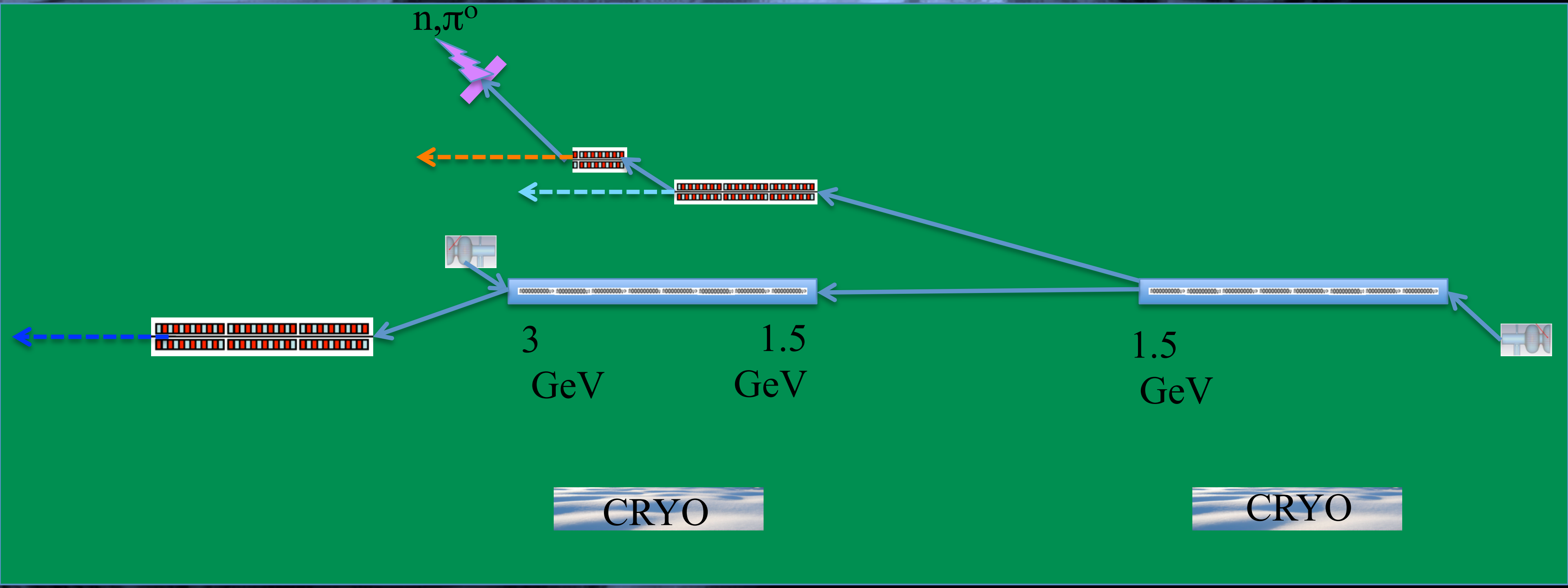

Neutron Source

This source may be suitable for multiple applications, ranging from material analysis for industrial and cultural heritages purposes to chip irradiation and metrology. These applications envisage the development of properly designed beam lines with neutron moderation and possibly cold/thermal neutron transport systems. The proposed new facility will represent a great opportunity for research and development of neutron instrumentation (e.g. detectors) as well as training of young scientist in the use and development of neutron techniques.

Deposited Power [kW]	Primary Electron Energy [GeV]	Expected Average Neutron Emission rate [n/s]
30	1	1.3 E+14
250	1	1.0 E+15
400	1	1.7 E+15
30	3	4.3 E+13
250	3	3.3 E+14
400	3	5.6 E+14

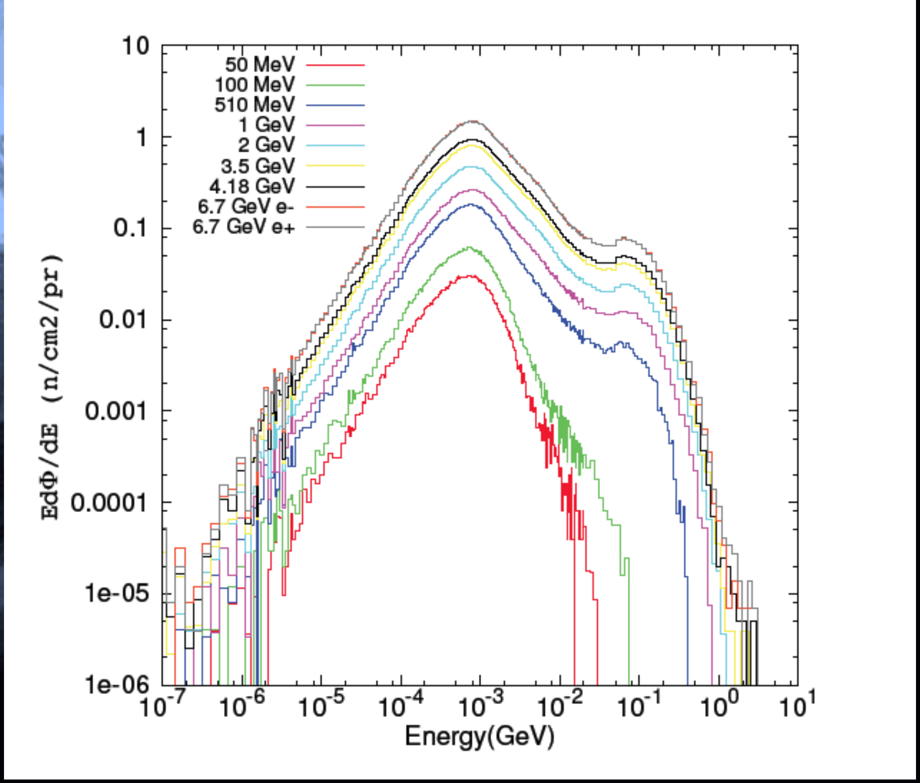

Comparison with other sources

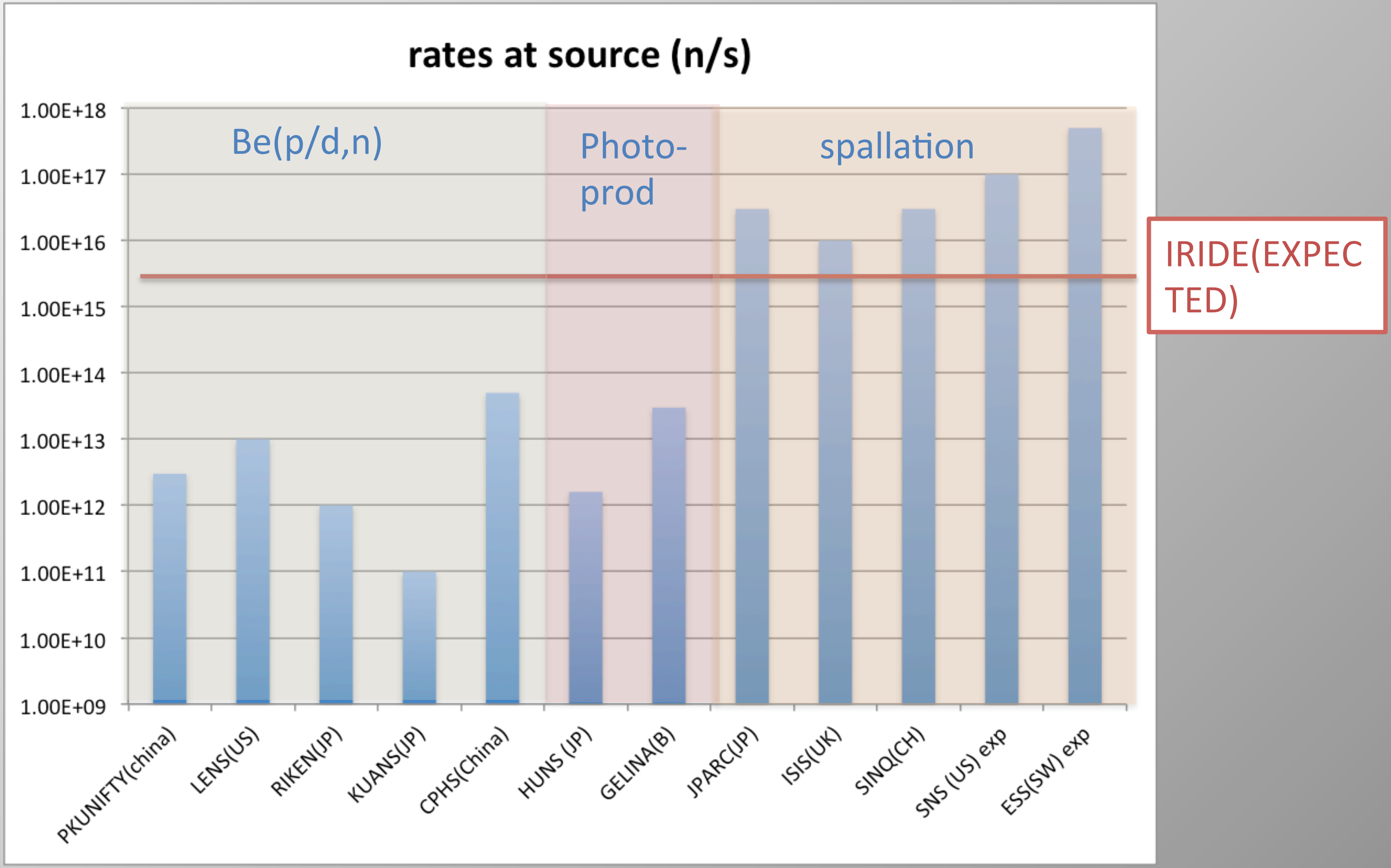

Neutron Source

Neutron Resonance Capture Analysis (NRCA): Each resonance is the fingerprint of a nuclear specie (isotopical recognition) thus allowing for the elemental material analysis (qualitative and quantitative) especially on metallic samples (e.g. cultural heritages).

Bragg Edge Transmission (BET): By means of this technique, stresses and strain in bulky samples can be analysed. This analysis is very important for both industrial as well as cultural heritages applications.

Chip irradiation : In order to test the robustness of electronic devices to neutron field in a few minutes, neutron beams produced at facilities are desirable as the may provide an almost atmospheric-like neutron spectrum but several order of magnitude more intense.

Radiography and Tomography (NR, NT): By means of radiography it is possible to obtain an image of a object that evidences the internal structure, by rotating the sample with respect to the incident beam and collecting images for each angular position a 3D image of the object is obtained (tomography).

Neutron metrology: In this context, the Italian National Institute of Ionization radiation Metrology (INMRI) is interested in having in Italy (and especially in Roma area) a high energy neutron source in order to develop primary standards for neutron emission rate and energy spectrum calibration

The special feature of Neutrograph is it's intensity together with a moderate collimation.

These properties allow the investigation of dynamic processes with an excellent time resolution and the transmittance through strongly absorbing and bulky materials.

A totally new spectrum of scientific and engineering applications could be developed.

Among the experiments are investigations of heat exchangers and combustion engines, parts from aircrafts, fossils and historical heritage.

Institut Laue-Langevin (ILL) in Grenoble

Advanced γ-ray Compton Source

The state of the art in producing high brilliance/spectral density mono-chromatic γ-ray beams will be soon enhanced, stepping up from the present performances (γ-ray beams with bandwidth nearly 3% and spectral density of about 100 *photons/s·eV*) up to what is considered the threshold for Nuclear Photonics, *i.e.* a bandwidth of the γ-ray beam lower than 0.3% and a spectral density larger than 10^4 *photons/s·eV*.

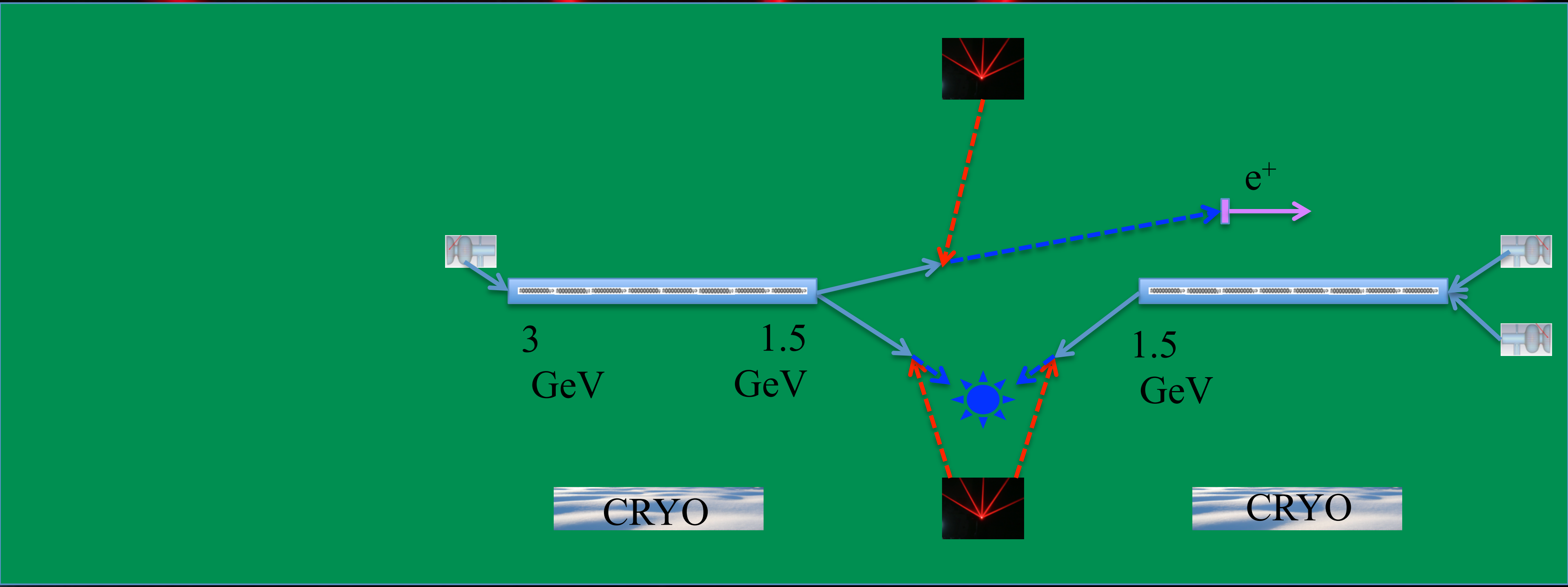

- colliding laser pulses to drive the back-scattering Compton (Yb:YAG, 100 W, 1 J, 0.1% bw)

Advanced γ-ray Compton Source

Parameters for ELI-NP case Recirculator	Units	Thomson Compton Source
Beam energy	[GeV]	1
Charge	[nC]	0.5
Bunch length rms	[μm]	300
Peak current	[A]	200
effective Rep. rate	[Hz]	60x100
Average current	[μA]	3
rms spot size at collision	[μm]	5
coll. Laser eff. Power	[kW]	0.1
coll. Laser pulse energy	[J]	1
rms norm. emittance	[μm]	0.5
beta-funct. at coll. (1 GeV)	[μm]	100
#γ/shot #γ/s	 $[s^{-1}]$	$6.0\ 10^{8}$ $3.6\ 10^{12}$

Parameters for SC-qCW case Fabry-Perot	Units	Thomson Compton Source
Beam energy	[GeV]	1
Charge	[nC]	0.5
Bunch length rms	[μm]	300
Peak current	[A]	200
Effective Rep. rate	[Hz]	9400x100
Average current	[μA]	470
rms spot size at collision	[μm]	5
coll. Laser eff. Power	[kW]	1000
coll. Laser pulse energy	[J]	0.01
rms norm. emittance	[μm]	0.5
beta-funct. at coll. (1 GeV)	[μm]	100
#γ/shot #γ/s	 $[s^{-1}]$	$6.0\ 10^{6}$ $5.6\ 10^{12}$

Advanced γ-ray Compton Source

- studies of the nucleus structure at the Pigmy and Giant Dipole Resonance with unprecedented resolution in reconstructing the nuclear states: this is crucial also to understand some unknown processes in the stellar nucleo-sinthesys

- studies of two level barionc states in the high energy resonance of the nuclei, above 20 *MeV* and up to 60 *MeV*, crucial to reconstruct the equation of state of the nuclear matter

- detection and imaging of fissile and strategic material with isotopic reconstruction of the components with large impact on the national security scenario

- remote sensing and diagnosys of nuclear wastes in containers, with reconstruciotn of the isoptope and nuclear composition of the waste material, with large impact on the atomic energy scenario

- medical imaging and therapy

γ-e Linear Collider

The precise measurement of the π^0 width through the process e $\gamma \rightarrow \pi^0$ e (*Primakoff effect*), and the search for light dark bosons in the energy region of few to hundreds MeV. These measurements, which provide important tests of the Standard Model, are not possible at present electron-photon colliders due to the low photon intensities of the machines.

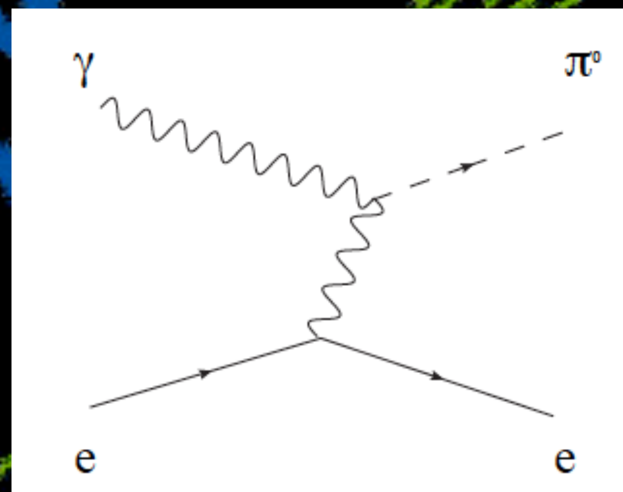

π^0 width measurement: the axial anomaly of Adler, Bell and Jackiw (non-conservation of the axial vector current) is responsible for the decay of the neutral pion into two photons. It bridges in QCD the strong dynamics of infrared physics at low energies (pions) with the perturbative description in terms of quarks and gluons at high energies. The anomaly allows to gain insights into the strong interaction dynamics of QCD and has received great attention from theorists over many years.

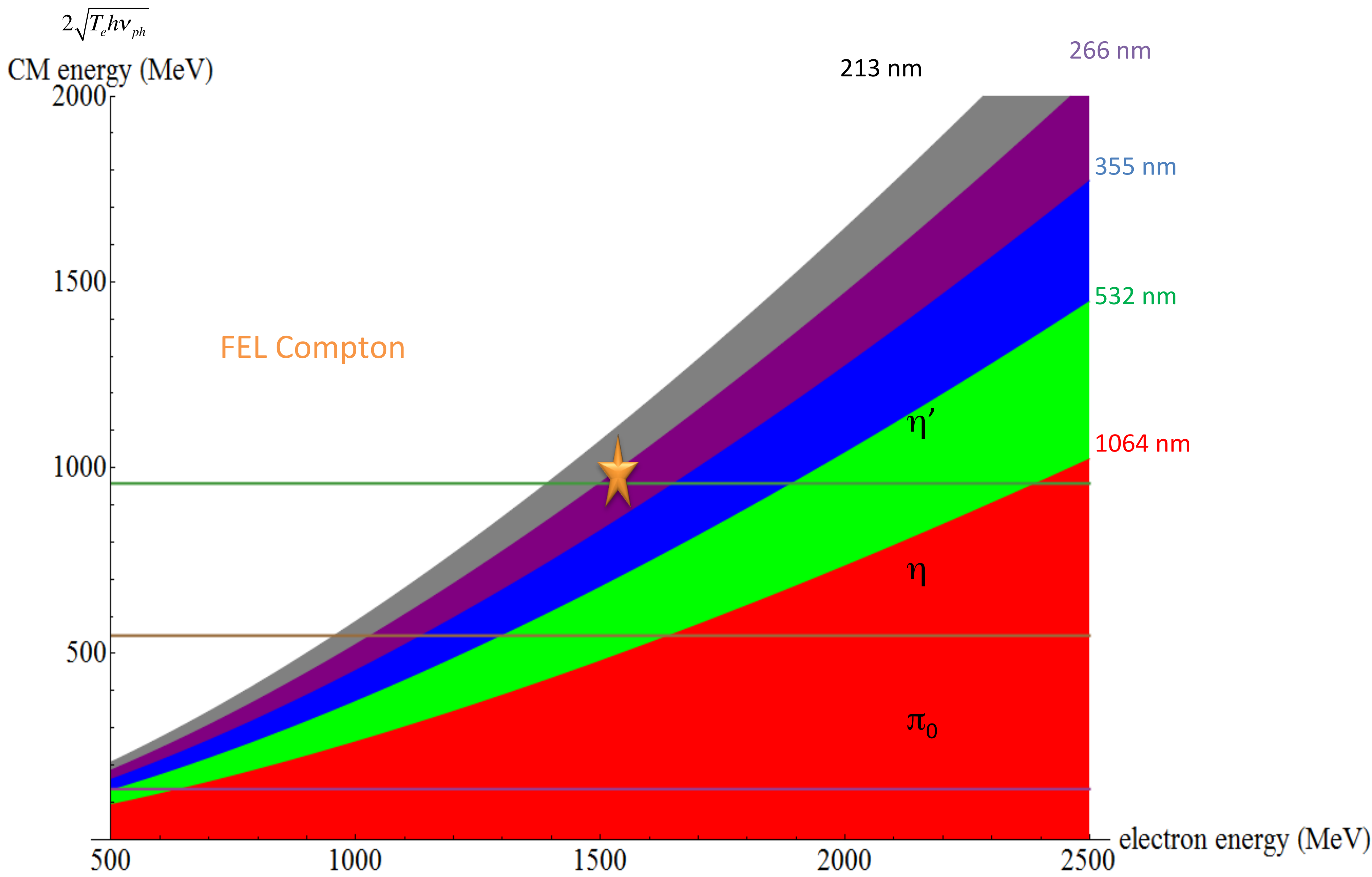

$2\sqrt{T_e h\nu_{ph}}$
CM energy (MeV)
2000
1500
1000
500
213 nm
266 nm
355 nm
532 nm
1064 nm
FEL Compton
η'
η
π_0
500
1000
1500
2000
2500
electron energy (MeV)

Intra-cavity Compton source driven by FEL oscillator

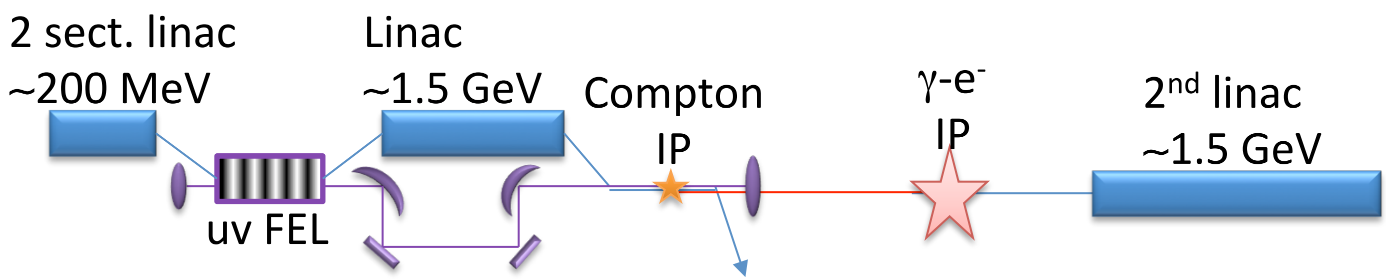

FEL Electron beam:

500 pC/bunch (5600 bunches/macrobunch for 0.28mA average current)
1ps length
Electron γ: 380 (200 MeV, 2 cryomodules)
Matched spot: 350um

FEL radiator:

Undulator period: 4.8 cm
Number of periods: 42 (201.6 cm)
Magnetic field on axis: 2.445 kG
FEL wavelength: 266 nm
Mirror loss: 3 10^{-4} (x12 pass./fel)
$K_U = 1.1$; $G_{MAX}*(1-\eta)/\eta = 181$
FEL intracavity intensity at saturation: 6.0 10^{12} W/cm^2
(23 mJ/pulse) s

Compton

\# of FEL pulse >0.95 FEL saturation: ~3950/ macrobunch
\# of $\gamma_{compton}$/shot: 3.4 10^6
Electron γ: 3050
Focus dimension: 5 um
$\gamma_{compton}$ energy: 153 MeV

γ-e^- interaction

Electron γ: 3050
CM energy: 977 MeV
IP dimension: 0.25 um
Luminosity: 0.5 10^{30} cm^{-2} s^{-1} (other sources 1.3 10^{30} cm^{-2} s^{-1} in 1st h) x0.25 in 2nd h, x0.09 in 3rd h

Conceptual scheme

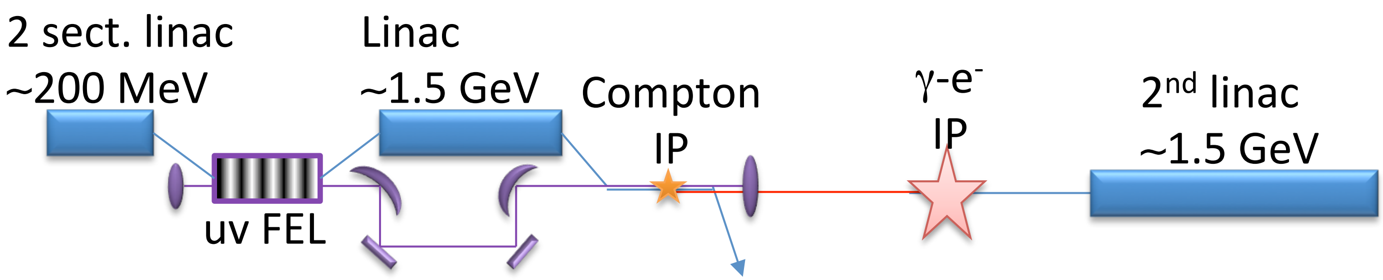

Yet to study:

- Electron beam characteristics after saturated FEL emission and dogleg
- Long two foci uv photon cavity
- Last mirror damage by Compton and synchrotron gamma radiation

γ-γ Linear Collider

The vacuum of QED poses some still unsolved challenges which are central not only in the context of field theory, but also of super-symmetry and string theory as well. The elastic photon-photon scattering offers unique opportunities to probe the nature of QED vacuum. We propose an experiment to observe photon-photon scattering in the range 1 MeV – 2 MeV CM energy, i.e., near the peak of the QED cross-section. In addition a low-energy photon-photon collider investigation could lead to the necessary technology developments and prepare the ground for a higher energy complex, while still providing a rich testing ground for QED, and, more generally, QFT.

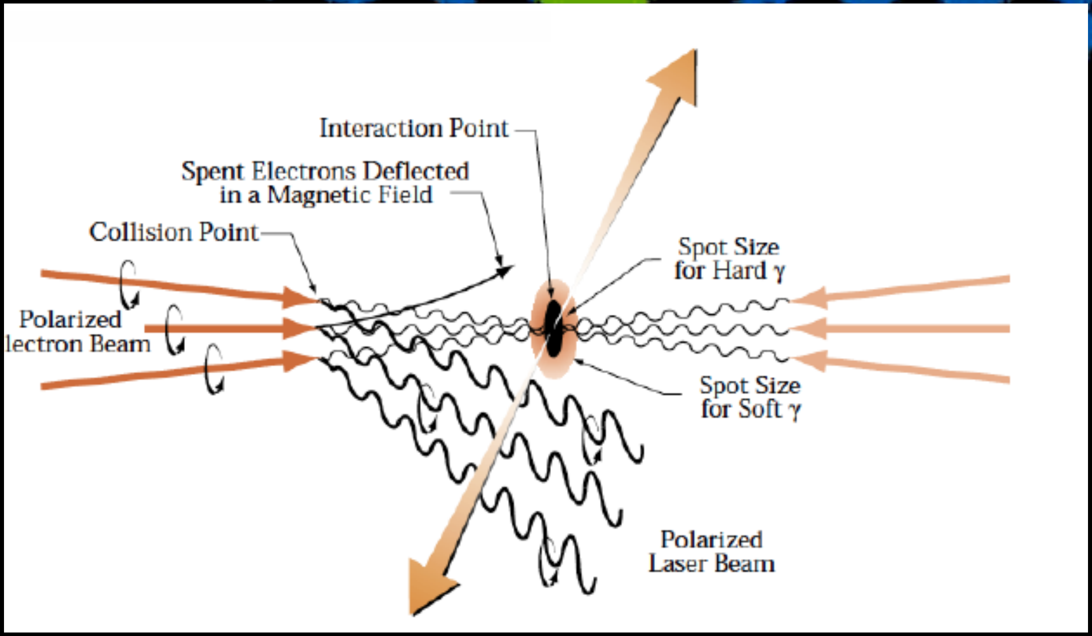

γ-γ Linear Collider

The most striking failing of QFT is the huge mismatch between the measured energy density of vacuum and the energy density of the ground level of the fundamental fields which is wrong by something like 120 orders of magnitude.

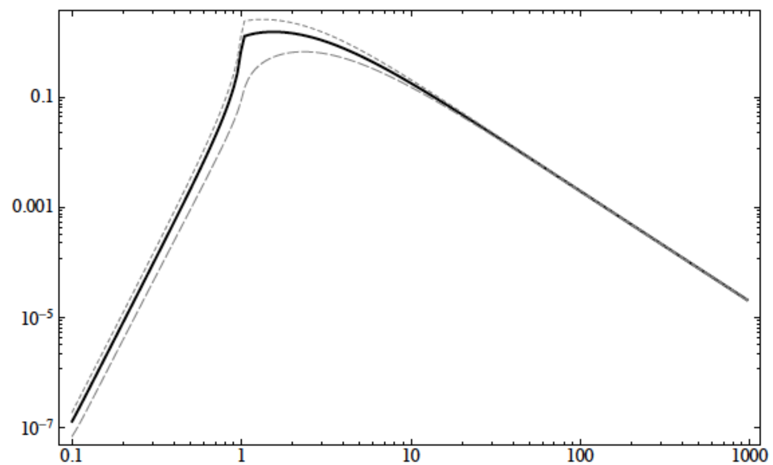

Figure 18: total cross-section (μbar) vs. CM energy (MeV). Solid line: cross-section averaged over initial photon polarizations. Dotted line: incoming photons have the same circular polarization. Dashed line: incoming photons have opposite circular polarization.

a photon-photon scattering experiment with photon energies in the 0.5-0.8 MeV range – where the cross-section is reasonably large, would be an important test of our understanding of the QED vacuum.

This experiment needs a low-energy photon-photon collider, and a photon detection apparatus which is very similar to that current PET scanners

Luminosity and beam requirements

Parameters for ELI-NP case	Units	Thomson Compton Source	γ-γ collider	e-γ collider
Beam energy	[GeV]	1	1	1
Charge	[nC]	0.5	0.5	0.5
Bunch length rms	[μm]	300	300	125
Peak current	[A]	200	200	1600
effective Rep. rate	[Hz]	60x100	60x100	60x100
Average current	[μA]	3	3	3
rms spot size at collision	[μm]	5	1	0.25
coll. Laser eff. Power	[kW]	0.1	0.1	0.1
coll. Laser pulse energy	[J]	1	1	1
rms norm. emittance	[μm]	0.5	1	1
beta-funct. at coll. (1 GeV)	[μm]	100	2	0.125
#γ/shot #γ/s	 [s^{-1}]	$6.0\ 10^{8}$ $3.6\ 10^{12}$		
Luminosity (coll)	[$cm^{-2}s^{-1}$]		$1.7\ 10^{28}$	$1.4\ 10^{30}$

Parameters for SC-qCW case	Units	Thomson Compton Source	γ-γ collider	e-γ collider
Beam energy	[GeV]	1	1	1
Charge	[nC]	0.5	0.5	0.5
Bunch length rms	[μm]	300	300	125
Peak current	[A]	200	200	1600
Effective Rep. rate	[Hz]	9400x100	9400x100	9400x100
Average current	[μA]	470	470	470
rms spot size at collision	[μm]	5	1	0.25
coll. Laser eff. Power	[kW]	1000	1000	1000
coll. Laser pulse energy	[J]	0.01	0.01	0.01
rms norm. emittance	[μm]	0.5	1	1
beta-funct. at coll. (1 GeV)	[μm]	100	2	0.125
#γ/shot #γ/s	 [s^{-1}]	$6.0\ 10^{6}$ $5.6\ 10^{12}$		
Luminosity (coll)	[$cm^{-2}s^{-1}$]		$2.7\ 10^{26}$	$2.2\ 10^{30}$

e^{+} e^{-} Linear Collider

An electron-positron collider with luminosity of 10^{32} $cm^{-2}s^{-1}$ with center of mass energy ranging from the mass of the φ-resonance 1 GeV up to ~3.0 GeV, would complement high-energy experiment at the LHC and future linear collider (ILC). Such a machine can easily collect an integrated luminosity of about 5 fb^{-1} in a few years of data taking.

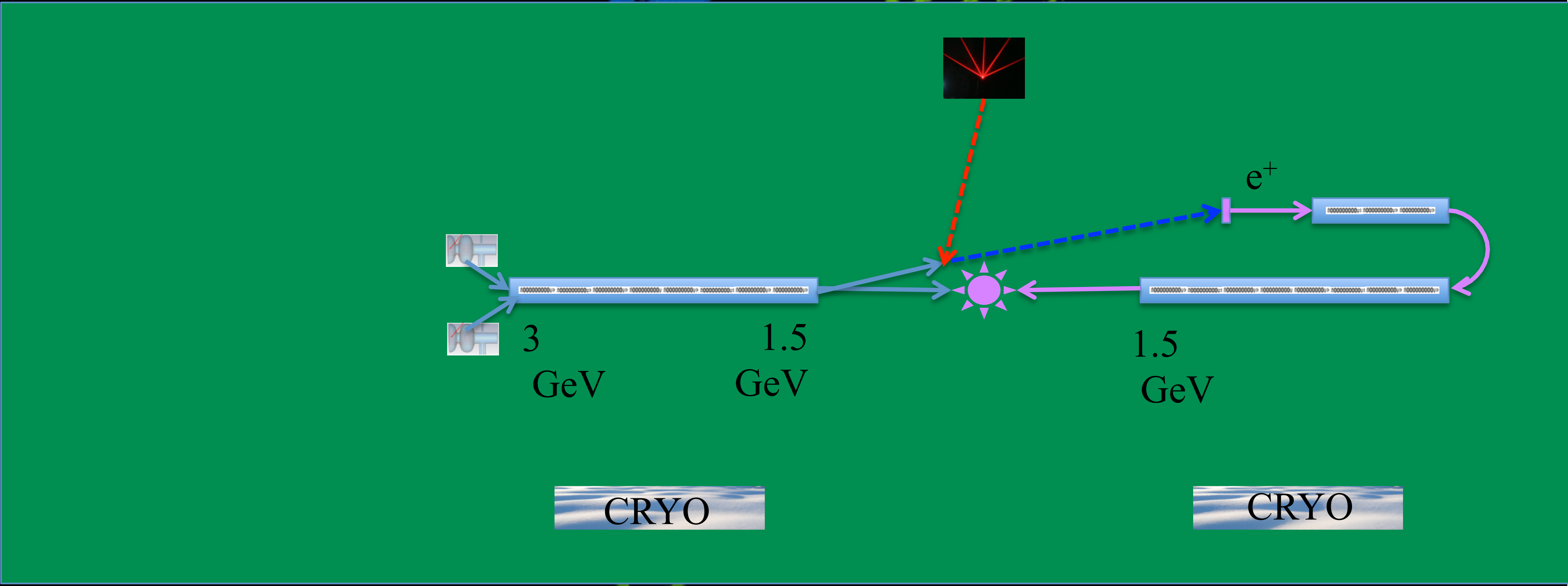

This will allow one to measure the $e^{+}e^{-}$ cross section to hadrons with a total fractional accuracy of 1%, a level of knowledge that has relevant implications for the determination of SM observables, like, the *g*-2 of the muon and the effective fine-structure constant at the M_Z scale. The latter are, through quantum effects, sensitive to possible bSM physics at scales of the order of hundred GeV or TeV.

e^+e^- collider

Physics opportunities with an e^+e^- collider with c.o.m. energy tunable within [~ 0.5, ~ 3.0] GeV

✓ hadronic cross-section meas. $e^+e^- \rightarrow \gamma^* \rightarrow$ had.

- hadronic contribution to muon a.m.m. a_μ
- hadronic contribution to α_{em}

✓ two-photon physics $e^+e^- \rightarrow e^+e^- \gamma^*\gamma^* \rightarrow e^+e^- +$ had.

- had. ≡ $\pi^0, \eta, \eta' \rightarrow$ light-by-light contribution to a_μ^{had}
- meson spectroscopy

✓ exotics $e^+e^- \rightarrow \gamma\, U \rightarrow \gamma\, \ell^+\ell^-$,
$\rightarrow \gamma\, E_{miss.}$

- possible existence of low-energy (0.1 ÷ 1 GeV) new gauge interactions (dark forces)

e⁺e- collider

LNF-10/17(P)

see also Eur. Phys. J. C **50** (2007) 729

Proposal for taking data with the KLOE-2 detector at the DAΦNE collider upgraded in energy

D. Babusci[a], C. Bini[b], F. Bossi[a], G. Isidori[a], D. Moricciani[c], F. Nguyen[d], P. Raimondi[a], G. Venanzoni[a], D. Alesini[a], F. Archilli[c], D. Badoni[a], R. Baldini-Ferroli[a,r], M. Bellaveglia[a], G. Bencivenni[a], M. Bertani[a], M. Biagini[a], C. Biscari[a], C. Bloise[a], V. Bocci[d], R. Boni[a], M. Boscolo[a], P. Branchini[d], A. Budano[d], S.A. Bulychjev[e], B. Buonomo[a], P. Campana[a], G. Capon[a], M. Castellano[a], F. Ceradini[d], E. Chiadroni[a], P. Ciambrone[a], L. Cultrera[a], E. Czerwinski[a], E. Dané[a], G. Delle Monache[a], E. De Lucia[a], T. Demma[a], G. De Robertis[f], A. De Santis[b], G. De Zorzi[b], A. Di Domenico[b], C. Di Donato[g], B. Di Micco[d], E. Di Pasquale[a], G. Di Pirro[a], R. Di Salvo[c], D. Domenici[a], A. Drago[a], M. Esposito[a], O. Erriquez[f], G. Felici[a], M. Ferrario[a], L. Ficcadenti[a], D. Filippetto[a], S. Fiore[b], P. Franzini[b], G. Franzini[a], A. Gallo[a], G. Gatti[a], P. Gauzzi[b], S. Giovannella[a], A. Ghigo[a], F. Gonnella[c], E. Graziani[d], S. Guiducci[a], F. Happacher[a], B. Höistad[h], E. Iarocci[a,i], M. Jacewicz[h], T. Johansson[h], W. Kluge[j], V.V. Kulikov[e], A. Kupsc[h], J. Lee Franzini[a], C. Ligi[a], F. Loddo[f], P. Lukin[k], F. Marcellini[a], C. Marchetti[a], M.A. Martemianov[e], M. Martini[a], M.A. Matsyuk[e], G. Mazzitelli[a], R. Messi[c], C. Milardi[a], M. Mirazzita[a], S. Miscetti[a], G. Morello[l], P. Moskal[m], S. Müeller[n], S. Pacetti[a,r], G. Pancheri[a], E. Pasqualucci[b], M. Passera[o], A. Passeri[d], V. Patera[a,i], A.D. Polosa[b], M. Preger[a], L. Quintieri[a], A. Ranieri[f], P. Rossi[a], C. Sanelli[a], P. Santangelo[a], I. Sarra[a], M. Schioppa[l], B. Sciascia[a], M. Serio[a], F. Sgamma[a], M. Silarski[m], B. Spataro[a], A. Stecchi[a], A. Stella[a], S. Stucci[l], C. Taccini[d], S. Tomassini[a], L. Tortora[d], C. Vaccarezza[a], R. Versaci[p],W. Wislicki[q], M. Wolke[h], J. Zdebik[m], M. Zobov[a]

e^+e^- - collider

Requests:

- ✓ luminosity $\sim 10^{32}\,\mathrm{cm}^{-2}\,\mathrm{s}^{-1}$
- ✓ energy $\sqrt{s} = (0.6 \div 3.0)\ \mathrm{GeV}$ (in steps of ~ 25 MeV)
- ✓ tagging systems for γγ-physics

Positron source ⟶ Bethe-Heitler: $\gamma Z \longrightarrow e^+e^- Z$

simulation (G4) in progress (collaboration w/ Rm2)

case under study: $E\gamma$ = 60 MeV on Pb (0.4 X_0)

e^- - target

✓ parity violating asymmetry meas. $e^{\uparrow\downarrow} Z \rightarrow e Z$

- Q^2-evolution of weak mixing angle θ_W

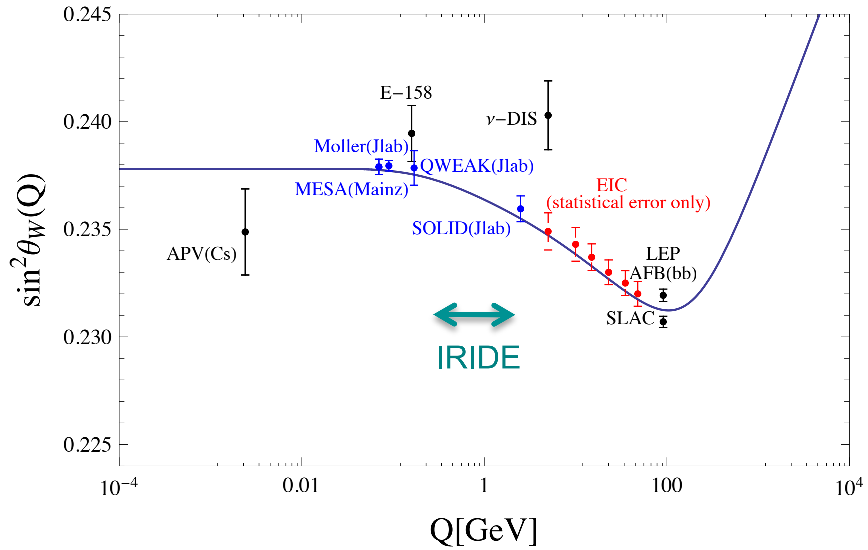

$$Q = \sqrt{y\, s}$$

$$\left(y = \frac{1 - \cos\theta_{cm}}{2} \right)$$

Requests: ✓ polarized beam (P ~ 90%; ΔP ~ 1%)

✓ average current > 200 μA

✓ dark forces searches $e Z \rightarrow e Z \mu^+\mu^-$

Table 12: Comparison between Conventional and ICS positron source performances

	Conventional	**ICS based**
RMS source size	400 μm	50 μm
N. particles/driving pulse	one 600 MeV electron	one 60 MeV photon
Target thikness	$6X_0$	$0.4X_0$
RMS transverse momentum	5 MeV	1 MeV
RMS emittance	0.001 m rad	$50*10^{-6}$ m rad
N. positrons/pulse	1	0.4

For the peak brightness the main advantage of driving the conversion directly with a photon beam relies on the possibility of using thinner targets. The emittance of the positron beam emerging from the target is determined by the source size and the beam divergence.

A primary effect of the electron-positron interaction is an enhancement of the luminosity due to the **pinch effect**, i. e. the reduction of the cross section of both beams occurring at the IP due to **self focusing forces** that is included in the luminosity definition through the factor $\mathbf{H_D}$.

$$L = \frac{n_b N_e^2 f_{rep}}{4\pi\sigma_x^* \sigma_y^*} \times H_D = \langle I \rangle \times \frac{N_e}{4\pi\sigma_x^* \sigma_y^*} \times H_D$$

$$H_D = \frac{L}{L^*} = \frac{\sigma_x^* \sigma_y^*}{\sigma_x \sigma_y}$$

$$D_{x,y} \equiv \frac{2N_e r_e}{\gamma} \frac{\sigma_z}{\sigma_{x,y}\left(\sigma_x + \sigma_y\right)}$$

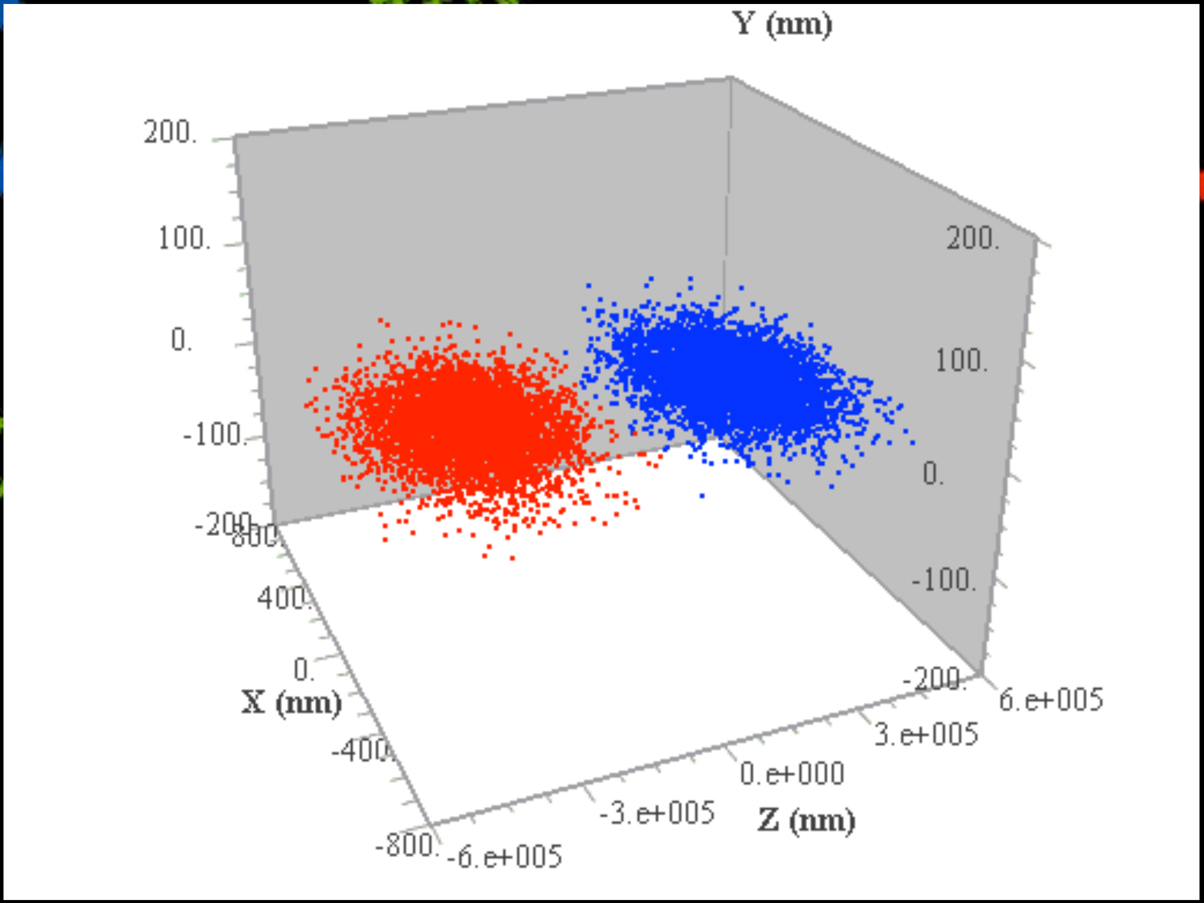

$$\sigma''_{pos,x} + \frac{k_{el}^2}{\gamma}\sigma_{pos,x} = \frac{\varepsilon^2_{pos,n}}{\gamma^2\sigma^3_{pos,x}}$$

$$k_{el}^2 = \frac{4I_{el}}{I_A\sigma^{*2}_{el,x}}$$

$$\sigma_{x,pos} = \sqrt[2]{\frac{\varepsilon_{n,pos}}{\sqrt{\gamma}k_{el}}}$$

Under the previous condition the positron beam spot size remains constant during the interaction due to the balance between its own defocusing emittance pressure and the counter-propagating electron beam focusing effect.

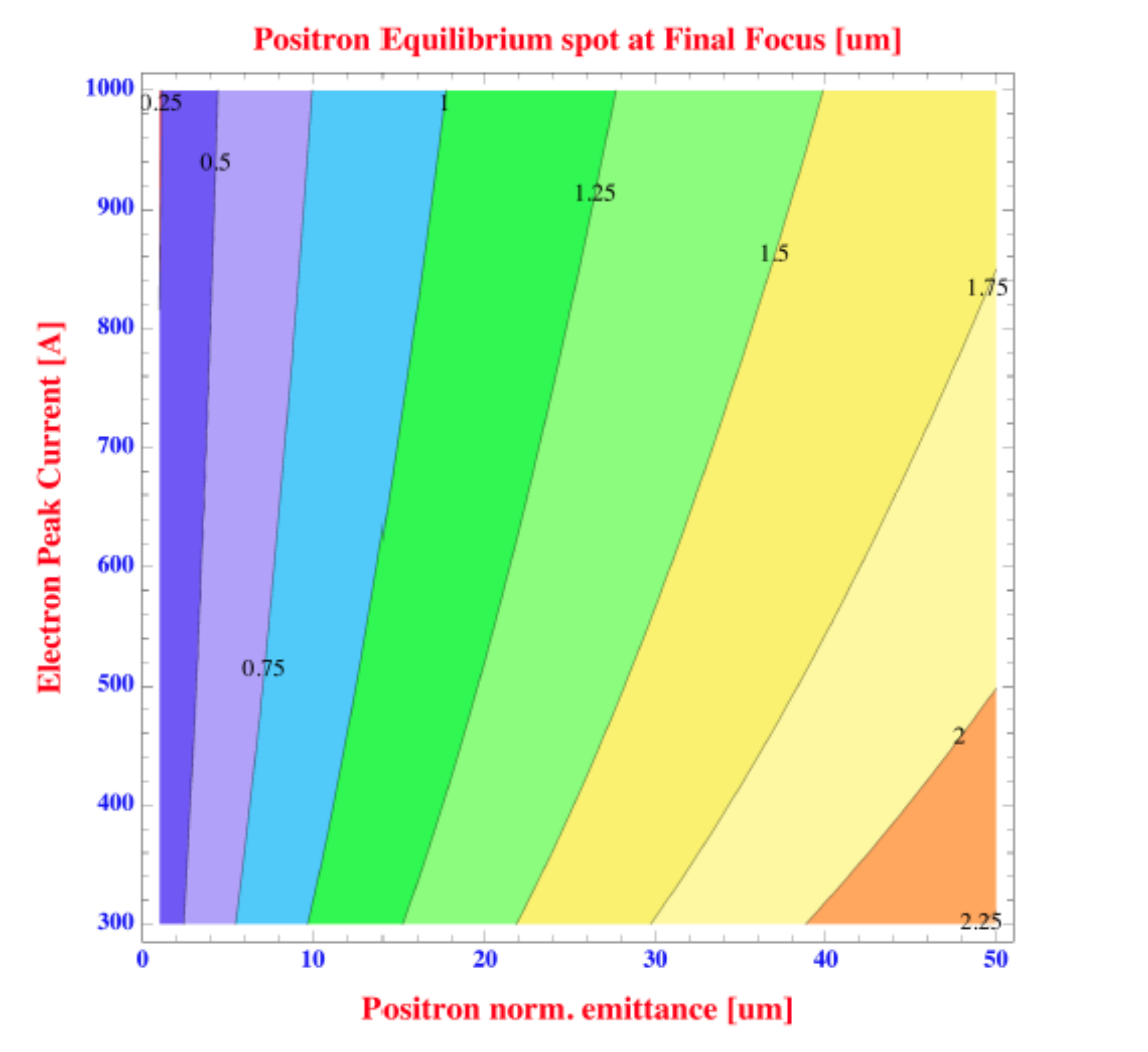

Parameters	Units	Electrons >< Electrons	Electrons >< Positrons	Reduced Positron quality
Beam energy	[GeV]	1	1	1
Beam power	[MW]	1	1	0.4
AC power	[MW]	1.9	1.9	1.3
Charge	[nC]	0.2	2	0.8
Bunch length rms	[μm]	500	675	450
Peak current	[A]	120	888	533
Rep. rate	[MHz]	5	0.5	0.5
Average current	[mA]	1	1	0.4
Transverse rms spot at IR	[μm]	0.5	1.5	1.5
Norm. emittance	[μm]	1	2	10
Beta at IR	[mm]	0.5	2.6	0.45
Aspect ratio	A	1	0.3	1
Disruption parameter	D	-3.5	5.3	1.4
Beam-strahlung parameter	δ_ε	$\sim 10^{-7}$	$\sim 10^{-7}$	$\sim 10^{-7}$
Luminosity enhancement factor	H_D	(<) 1	5.8	1.3
Luminosity	$cm^{-2}s^{-1}$	$\sim 2.5\ 10^{32}$	$1.6\ 10^{33}$	$\sim 1.1\ 10^{32}$

IRIDE road map

- March –> June – Working Groups Meeting with int. experts
- July 31 – White Book ready
- By the end of 2013 IRIDE approval?


Thank you